

Research Article

Numerical Simulation of the Performance of a Twin Scroll Radial Turbine at Different Operating Conditions

Carlo Cravero , Davide De Domenico, and Andrea Ottonello

Dipartimento di Ingegneria Meccanica, Energetica, Gestionale e dei Trasporti (DIME), Università degli Studi di Genova, Genova 16145, Italy

Correspondence should be addressed to Carlo Cravero; cravero@unige.it

Received 2 January 2019; Revised 12 March 2019; Accepted 7 April 2019; Published 2 June 2019

Academic Editor: Ryoichi Samuel Amano

Copyright © 2019 Carlo Cravero et al. This is an open access article distributed under the Creative Commons Attribution License, which permits unrestricted use, distribution, and reproduction in any medium, provided the original work is properly cited.

Twin scroll radial turbines are increasingly used for turbocharging applications, to take advantage of the pulsating exhaust gases. In spite of its relevance in turbocharging techniques, scientific literature about CFD applied to twin scroll turbines is limited, especially in case of partial admission. In the present paper a CFD complete model of a twin scroll radial turbine is developed in order to give a contribution to literature in understanding the capabilities of current industrial CFD approaches applied to these difficult cases and to develop performance index that can be used for turbine design optimization purposes. The flow solution is obtained by means of ANSYS CFX[®] in a wide range of operating conditions in full and partial admission cases. The total-to-static efficiency and the mass flow parameter (MFP) have been calculated and compared with the experimental database in order to validate the numerical model. The purpose of the developed procedure is also to generate a database for twin scroll turbines useful for future applications. A comparison between performances obtained in different admission conditions was performed. In particular the analysis focused on the characterization of the flow at volute outlet/rotor inlet section. A flow distortion index at rotor inlet was introduced to correlate the turbine performance and the flow nonuniformities generated by the volute. Finally the influence of the backside cavity on the performance parameters is also discussed. The introduction of these new nonuniformity indices is proposed for volute design and optimization procedures.

1. Introduction

Radial turbines are gaining an increasing importance in several engineering applications. In energy generation they are widely used in micropower plants [1–3], often coupled with thermal energy generation for cogenerative purpose. Another common and well-established application field is turbocharging: as a part of downsizing engine strategy in order to decrease greenhouse gas emissions, maintaining high specific power levels. Among possible turbocharging schemes, pulse turbocharging is a convenient solution for the possibility of taking advantage of the pressure periodic fluctuations (generated by the periodic opening of the engine discharge valves) by mean of exhaust manifolds characterized by small diameters and lengths (low damping volume). However, this technique introduces issues related to the possible interaction of pressure waves coming from different cylinders and to periods of windage, which can mitigate the

positive effect of pulsating flow. Considering that the mass flow passing through the turbine in pulsating condition is lower than the stationary one, in order to make the gas supply to the turbine as homogeneous as possible (thus optimizing the performance of the turbine), it is important to group the cylinders exhausts into different manifolds. The main problem in pulse turbocharging is the choice of which cylinders have to be connected together. As known in a four-stroke engine the discharge phase lasts approximately 240° of crank angle. In order to avoid the interaction among different cylinders during exhaust valves opening, they should be linked so that the firing sequences are shifted by a crank angle equal (six cylinders engine) or greater than 240° [4].

Pulse turbocharging leads often to the application of peculiar turbine volute geometries, such as twin scroll or double entry types. In a double entry configuration the inlets create two separated admission channels which feed different sectors of the rotor in circumferential direction. In twin scroll

turbines the inlet is meridionally divided into two limbs (hub and shroud rotor sides), but in this case both of them feed the entire rotor circumference [5].

Flow investigation of such solutions is increasingly important because of complex fluid-dynamic phenomena and strong 3D flow structures. A better understanding of the turbine flow field under different admission conditions can be useful for the matching with the internal combustion engine. As an example, Dale and Watson [6] experimentally demonstrate that, even if the two limbs of a twin scroll turbine are symmetrical and the mass flow rates from inlets are almost coincident, highest values of efficiency are reached when the shroud limb flow rate is greater than the one passing through the hub branch. Several works also investigate turbines performances under steady and unsteady flow conditions [5, 7–9].

The backside cavity behind the rotor disk can affect the flow at rotor inlet and consequently turbine performance. The flow features within the cavity were investigated by Raetz et al. [10] to calculate aerodynamic forces in a turbocharger. Results showed a flow structure with high total pressure gradients in the radial direction generated by centrifugal forces.

The prediction of twin and double entry radial turbine performance for turbocharging applications in a wide range of operating conditions requires the adoption of 3D CFD models. Newton et al. [11] simulated a double entry turbine with the purpose to investigate the source of losses in full and partial admission. They divided the computational analysis in two parts: the full admission condition was simulated with a single channel in steady-state conditions, whereas the complete rotor was considered for partial admission unsteady simulation. Shahhosseini et al. [12] proposed a three-dimensional CFD model based on Favre-averaged Navier Stokes equations (FANS), using a finite volume method. This model gives a more useful form of equations for compressible flows and was used to analyze performances in full and partial admission; the results were also compared to experimental data obtained by Shahhosseini et al.

Xue et al. [13] developed a procedure by using Ansys CFX® commercial code for the study of twin entry turbines losses. They meshed the volute by tetrahedral elements whereas the rotor was discretized with a structured grid. They used steady-state RANS equations with SST model for turbulence closure. Total pressure and temperature were set as inlet boundary conditions; average static pressure was fixed at the outlet. Xue et al. obtained a good match between experimental and numerical data. They compared various different admission conditions in order to investigate loss contribution of each turbine component.

A CFD model for a twin scroll radial turbine was set up by the authors [14] focusing on the investigation of volute performances. The above model was simplified by adopting a single rotor channel configuration. The rotor was included to fix the operating point and the investigations concerned the volute performance.

Published papers can be found in literature with detailed CFD investigations of twin scroll and double entry turbines. However, except from Xue et al. who depicted and commented the flow distortion at the rotor inlet of a vaned

TABLE I: Volute geometrical parameters.

Geometric parameter	Value
<i>Radial extension vaneless distributor</i>	0.0252 [-]
<i>Volute area ratio</i> ($AR = A_2 / A_{1\text{tot}}$)	0.910 [-]
A_2/r_2	54.0 [mm]
$A_{1\text{hub}}/r_{1\text{hub}}$	9.33 [mm]
$A_{1\text{sh}}/r_{1\text{sh}}$	16.2 [mm]

turbine, none of the other authors investigated the flow field at the impeller inlet and suggested volute performance indices.

In the current paper a CFD model (volute and full rotor) for a complete twin scroll radial turbine has been considered. Simulations were performed with and without backside cavity in a wide range of operating points at both full and partial admission. The CFD model has been validated with experimental data. A comparison of performance parameters (total-to-static efficiency and MFP) for different admission cases is discussed with the help of flow nonuniformity indices. These are presented as possible volute performance parameters to be used to compare volute designs or in an automatic design optimization procedure.

2. Reference Geometry

The test case turbine is a twin scroll radial inflow turbine for turbocharging applications. Geometrical data are confidential; then all quantities have been reported in nondimensional or reduced form. The same geometry was used in a previous work [14].

2.1. *Volute.* The geometrical parameters of the volute are listed in Table 1:

- (i) radial extension of vaneless distributor, which has been made nondimensional with $r_{1\text{sh}}$;
- (ii) volute area ratio that compares outlet volute area (A_2) and total inlet area ($A_{1\text{sh}} + A_{1\text{hub}}$);
- (iii) area to radius ratios (A/r).

Since the examined turbine is twin scroll, the volute has two inlet sections connected to exhaust manifolds (Figure 2). They are defined according to their relative position with respect to the rotor: hub side inlet (i) and shroud side inlet (ii).

2.2. *Rotor.* The geometrical data are summarized in Table 2.

Figure 1(a) shows the position of the main parameters on a reference sketch of a generic turbine section.

The impeller (Figure 1(b)) is composed by $z_b = 9$ blades with a radial leading edge ($\beta_{b2} = 0^\circ$) and outlet metal angle β_{b3} increasing with radius in order to match peripheral velocity variation at the trailing edge.

A peculiar feature of the radial machine is the backside cavity; it consists of the volume between the backside (rotating circular surface behind the impeller) and the stationary housing. A meridional section of this geometrical detail is shown in Figure 1(b).

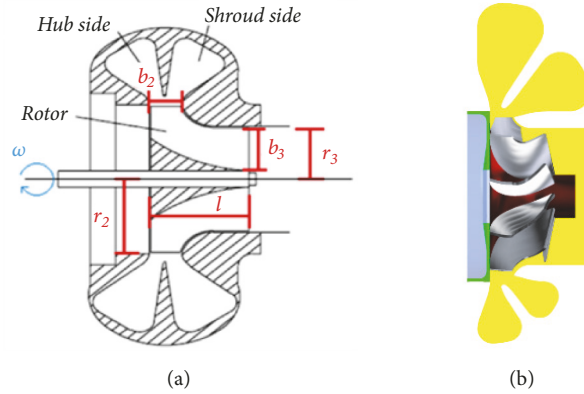


FIGURE 1: (a) Sketch of meridional section of a generic twin scroll turbine; (b) rotor view with a cut of the volute and housing with the backside cavity (in green).

TABLE 2: Rotor geometrical dimensionless parameters.

Geometric parameter	Value
Inlet blade height (b_2)	0.299
Outlet blade height (b_3)	0.572
Outlet blade radius (r_3)	0.843
Rotor axial size (l)	0.829
Tip clearance	0.0199
Inlet blade thickness	0.0361
Outlet blade thickness (shroud)	0.0675
Outlet blade thickness (hub)	0.0359

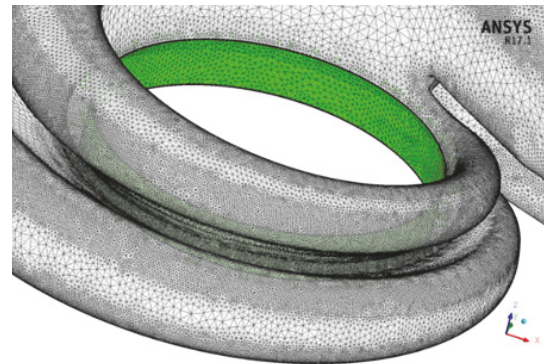


FIGURE 3: Unstructured grid detail on the two volute branches (shroud side the upper and hub side the lower). In green is highlighted the volute outlet section, which feeds turbine rotor.

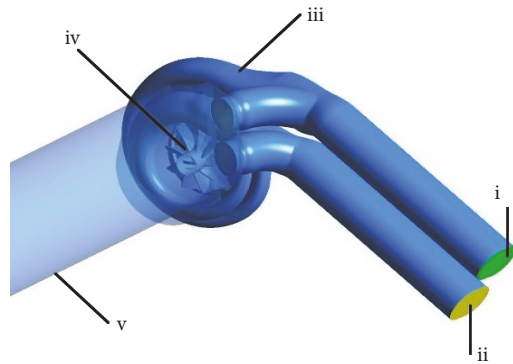


FIGURE 2: Turbine CFD domain: (i)-(ii) inlet sections, (iii) volute domain, (iv) rotor domain, and (v) out domain.

In the first part of the paper the geometrical model does not include the cavity. In the second part (from Section 7) the feature is included in the model.

3. CFD Model

The ANSYS® CFX numerical platform has been used. The twin scroll volute is discretized with an unstructured mesh

(viscous mesh layers added), as depicted in Figure 3, while a structured grid is generated for the rotor (Figure 4). Special attention was paid to the accurate resolution of the boundary layer on the walls by means of ten prism layers with exponential clustering to the wall. In order to avoid the use of wall functions, the height of the first layer has been calculated to get y^+ close to one.

The model is divided into three domains (Figure 2):

- (i) volute
- (ii) rotor
- (iii) out

Simulations were performed with steady flow condition. The above choice is due to the comparison of steady-state CFD performance with the corresponding experimental data that were not obtained matching the turbo with an internal combustion engine, but at a gas stand test bench. Boundary conditions set for the different domains are reported in Table 3; these are valid for the full admission condition.

In partial admission, one of the two limbs is closed; this situation was simulated by introducing a wall boundary for the inlet (zero mass flow).

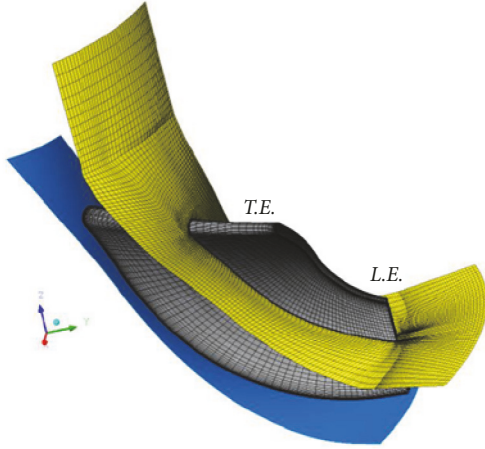


FIGURE 4: Rotor channel structured mesh.

TABLE 3: Boundary conditions.

Volute	Rotor	Outlet
Total pressure and total temperature, different for each inlet (hub or shroud)	Rotational speed	Static Pressure on outlet section
Flow direction orthogonal to volute inlet sections	Shroud wall counter-rotating with respect to blades	-
Inlet turbulence intensity 5%		

Experimental data for inlet total conditions, outlet static pressure, and rotational speed are used as boundary conditions.

The compressible flow model consists in Reynolds Averaged Navier Stokes (RANS) equations; the Shear Stress Transport (SST) model for turbulence closure was adopted because of its higher accuracy and calibration in the code for turbomachinery applications. The equations have been solved with the High Resolution scheme that has second-order accuracy.

The SST takes into account the transport of the turbulent tangential stresses, providing very accurate predictions on the trigger and degree of flow separation under adverse pressure gradients.

The fluid is a perfect gas with a specific heat $C_p=1.15$ [kJ/(kg*K)] and a dynamic viscosity which varies with temperature according to Sutherland law.

$$\mu = \mu_{ref} \left(\frac{T}{T_{ref}} \right)^{3/2} \frac{T_{ref} + Su}{T + Su} \quad (1)$$

4. Turbine Performance Parameters

This paragraph deals with the definition of performance parameters and reference nondimensional or reduced quantities used to set turbine operating point:

- (i) pressure ratio flow (PRF) is the ratio between the total pressure at volute inlet (p_{t1}) and static exit pressure (p_{ex}). In full admission the inlet total pressure corresponds to an arithmetical mean of inlets total pressures (p_{t1hub} , p_{t1sh}). In partial admission instead, PRF is considered as the ratio between the total pressure of the fed branch and outlet static pressure;

$$PRF = \frac{p_{t1}}{p_{ex}} \quad (2)$$

- (ii) reduced rotational speed is the ratio between turbine rotational speed and the square root of the inlet total temperature (T_{t1});

$$N_{red} = \frac{N}{\sqrt{T_{t1}}} \quad (3)$$

- (iii) mass flow parameter (MFP) is used to estimate turbine flow capacity and its equation is reported below in the modified version without the reference geometric area (see [7]):

$$MFP = \dot{m} \frac{\sqrt{T_{t1sh} * MFR_{sh} + T_{t1hub} * MFR_{hub}}}{p_{t1}} \quad (4)$$

where MFR is the ratio between the amount of mass flow passing through the considered limb and overall mass flow processed by the turbine;

$$MFR_i = \frac{\dot{m}_i}{\dot{m}} \quad (5)$$

- (iv) total-to-static efficiency is the ratio between the ‘real’ total enthalpy drop and the amount of energy obtainable from the turbine with an isentropic process:

$$\eta_{ts} = \frac{1 - (T_{t1}/T_{t3})}{1 - (1/PRF)^{((k-1)/k)}} \quad (6)$$

The total inlet conditions are mass flow averaged values on the reference sections. Static pressure is an area averaged value on the reference section.

5. Experimental Validation

Table 4 presents the set of pressure ratios considered for the different rotational speeds and admission conditions.

Twin scroll turbines can operate in different conditions:

- (i) partial admission \rightarrow zero mass flow in one of the limbs. The case studied with mass flow only in shroud side branch was called “partial shroud”, while in the opposite case was called “partial hub”;
- (ii) full admission \rightarrow both volute branches are fed approximately by the same exhaust gas mass flow (differences due to asymmetry of the two sectors and the different boundary conditions applied).

TABLE 4: Set of tested cases in full, partial shroud, and partial hub admission.

full		partial shroud		partial hub	
N	PRF	N	PRF	N	PRF
$[rpm/(K^{0.5})]$		$[rpm/(K^{0.5})]$		$[rpm/(K^{0.5})]$	
N1	1.31	N1	1.56	N1	1.51
	1.37		1.69		1.62
	1.42		1.77		1.69
N2	1.79	N2	2.35	N2	2.18
	1.99		2.72		2.51
	2.15		2.99		2.76
N3	2.54	N3	3.34	N3	3.15
	2.83		3.72		3.49
	3.15		4.35		3.93

TABLE 5: Percentage difference for MFP values.

N	PRF	$MFP_{\%diff}$
N1	1.31	3.53
	1.37	3.34
	1.42	3.18
N2	1.79	2.98
	1.99	2.60
	2.15	2.35
N3	2.54	3.33
	2.83	2.85
	3.15	2.98

In this work partial and full admissions were simulated.

Nine operating points have been chosen over three different isospeeds in order to properly cover the turbine working range.

The values of the mass flow parameter (MFP) and of the total-to-static efficiency calculated from the CFD simulations are compared to the corresponding experimental data. In the following paragraphs the different admission cases are discussed separately.

5.1. Full Admission Validation. Full admission results are compared in Figures 5-6 with experimental data. From the comparison among ‘MFP vs PRF’ trends, it can be noticed that there is a good match between experimental and numerical data (values are very close), with the CFD which tends to slightly underestimate the mass flow rate. The MFP percentage difference (see (7)) between CFD and experimental values is generally below 3.5% (see Table 5).

Figure 6 shows total-to-static efficiency trends. For confidentiality reasons efficiency values are not reported. It can be noticed that

- (i) CFD tends to overestimate efficiency values;
- (ii) CFD and experimental data trends are different: numerical results show a trend that is monotonically decreasing with the PRF whereas the experimental data have a peak.

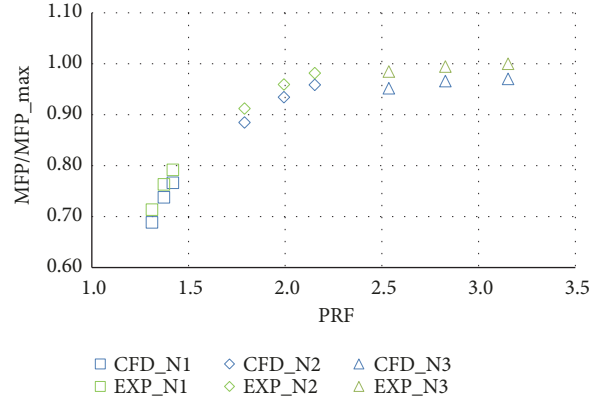
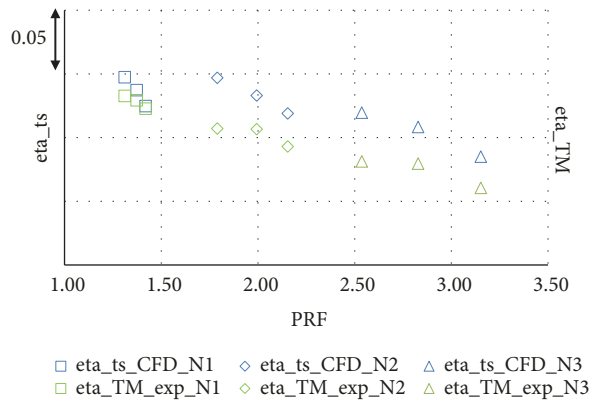


FIGURE 5: MFP (referred to maximum value) vs PRF in full admission, CFD (blue) and experimental data (green).

FIGURE 6: η_{ts} vs PRF in full admission, CFD (blue) and experimental data (green).

This difference in trends can be mainly explained considering mechanical efficiency.

It must be noticed that while CFD efficiency is obtained with (6), the experimental data refer to the ‘‘turbine effective efficiency’’ (thermomechanical performance), which includes the mechanical losses, leading to lower values of the performance index.

Moreover turbine mechanical efficiency depends on operating point [15, 16] and its behaviour can explain the trend mismatch between CFD and experimental data. However the mean percentage difference is below 4%.

$$\text{percentage diff.} = \frac{|MFP_{CFD} - MFP_{EXP}|}{MFP_{EXP}} 100 \quad (7)$$

5.2. Partial Shroud Admission Validation. In case of partial shroud admission the hub limb is completely closed. The performance comparison in Figure 7 shows that in this case the CFD model slightly overestimates experimental MFP values (the opposite occurs in Figure 5 for full admission).

The numerical error is quantified for the operating points in Table 6.

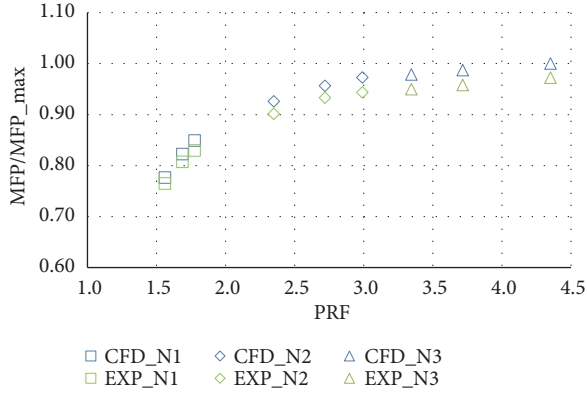


FIGURE 7: MFP (referred to maximum value) vs PRF in partial shroud admission, CFD (blue) and experimental data (green).

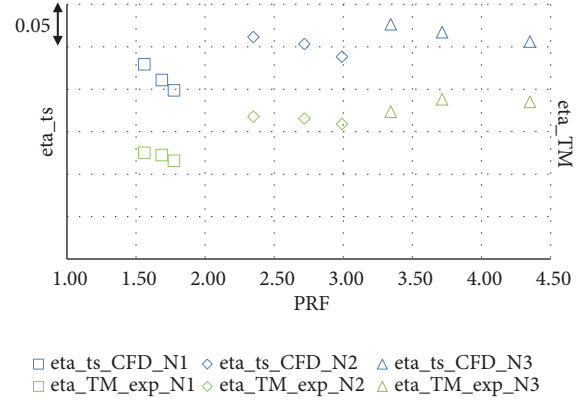


FIGURE 8: η_{ts} vs PRF in partial shroud admission, CFD (blue) and experimental data (green).

TABLE 6: Percentage difference for MFP values.

N	PRF	MFP_%.diff
N1	1.56	1.55
	1.69	1.87
	1.77	2.35
N2	2.35	2.71
	2.72	2.53
	2.99	3.12
N3	3.34	3.05
	3.72	3.02
	4.35	2.84

The CFD model tends to overestimate experimental data for the total-to-static turbine efficiency, as in full admission. In this case the average error is higher and about 15% (Figure 8).

5.3. Partial Hub Admission Validation. In this case the shroud limb is closed and only the hub branch is fed by exhaust gas. The comparison between numerical and experimental data gives results similar to partial shroud condition. MFP (Figure 9) and η_{ts} (Figure 10) are both overestimated by the CFD model.

The error for mass flow parameter estimation is reported in Table 7, while the discrepancy between CFD and experimental data for total-to-static efficiency is about 20%.

$$\alpha_{index} = \frac{1}{(n.v. * \bar{\alpha})} * [0.1 |\alpha_{10} - \bar{\alpha}| + 0.25 |\alpha_{25} - \bar{\alpha}| + 0.5 |\alpha_{50} - \bar{\alpha}| + 0.75 |\alpha_{75} - \bar{\alpha}| + 0.9 |\alpha_{90} - \bar{\alpha}|] \quad (8)$$

Figure 11 shows that in partial shroud admission MFP is lower than in the opposite case (partial hub).

Even though the assigned boundary conditions are very similar in the partial cases, the mass flow distribution between shroud and hub volute branches is different, due to the strong geometrical asymmetry of the two scrolls of this radial turbine.

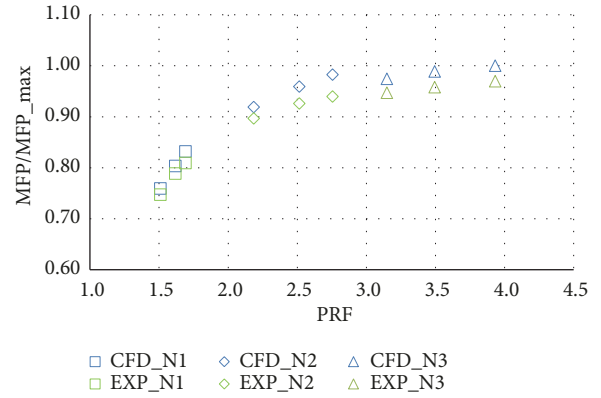


FIGURE 9: MFP (referred to maximum value) vs PRF in partial hub admission, CFD (blue) and experimental data (green).

TABLE 7: Percentage difference for MFP values.

N	PRF	MFP_%.diff
N1	1.51	1.62
	1.62	1.85
	1.69	2.76
N2	2.18	2.44
	2.51	3.58
	2.76	4.56
N3	3.15	2.90
	3.49	3.23
	3.93	3.12

6. Performance Analysis

The database of CFD simulations can also be used to compare twin scroll turbine performance in various admission conditions. As already remarked by the authors in previous papers [14], full and partial admission cases cannot be compared with each other because the mass flow rate in full admission is approximately twice the one in partial admission.

In order to identify the volute performance for the different operating conditions, a performance index [14] has

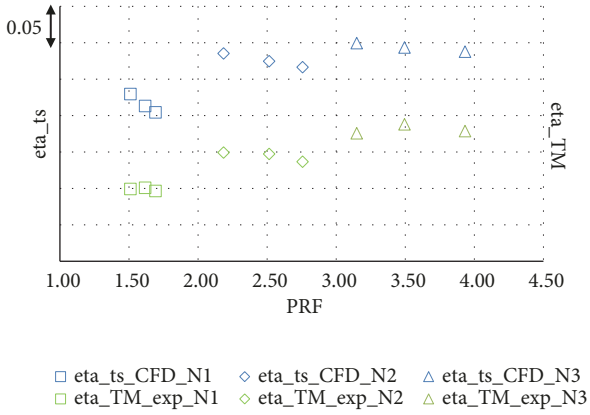


FIGURE 10: η_{ts} vs PRF in partial hub admission, CFD (blue) and experimental data (green).

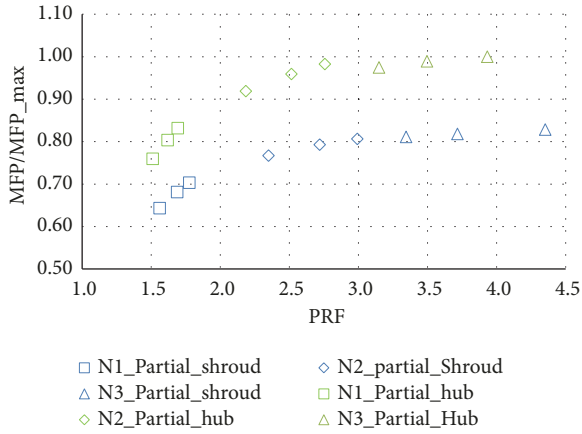


FIGURE 11: MFP (referred to maximum value) vs PRF, partial shroud (blue) and partial hub (green).

been defined to highlight the flow nonuniformity at rotor inlet. It is called α_{index} and calculated as follows.

The abovementioned index is obtained considering the absolute flow angle α distribution along the span from hub to shroud. $\bar{\alpha}$ is the mean value of the flow angle in stationary frame at rotor inlet, while α_n corresponds to the flow angle at the n-th percentage of the span (starting from the hub towards the shroud). This index is defined as a span position weighted average of local α deviation from mean value. The flow angle spanwise trend at rotor inlet section changes significantly by varying admission condition: in full admission case (Figure 12) α is almost constant for most of the span (up to 80%), but near the shroud there is a remarkable decrease.

In partial shroud conditions the trend is similar to the full case with a higher decrease at the shroud side (Figure 13). On the contrary, the partial hub case shows a different α variation through the span (Figure 14) with a localized increase near the shroud. Since the alpha index was developed with the purpose to evaluate turbine volute performance, the model that was adopted for this analysis did not include the rotor

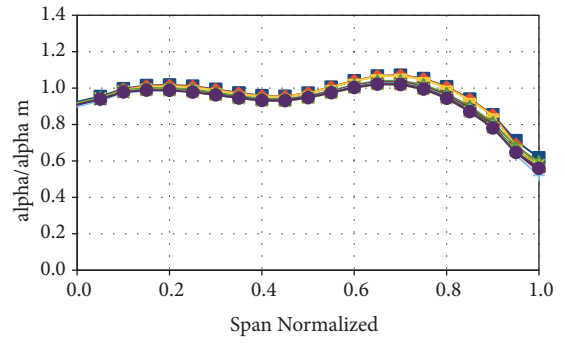


FIGURE 12: Flow angle/mean flow angle vs span at rotor inlet section for different rotational speed, full admission.

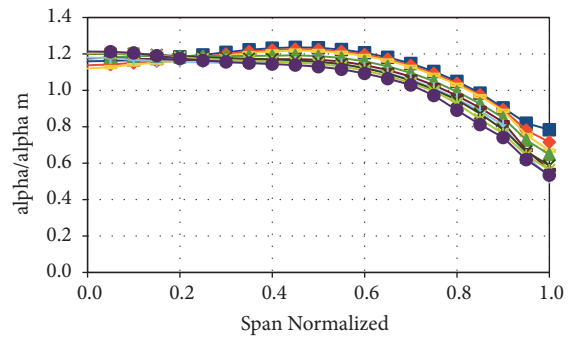


FIGURE 13: Flow angle/mean flow angle vs span at rotor inlet section for different rotational speed, partial shroud admission.

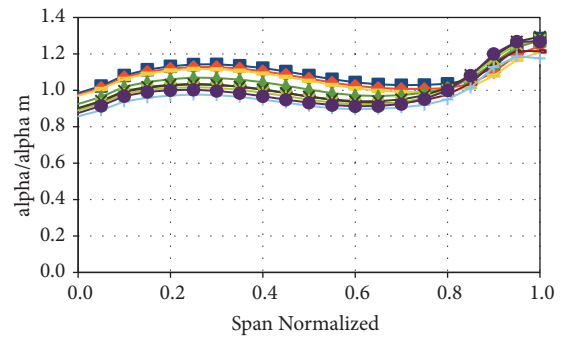


FIGURE 14: Flow angle/mean flow angle vs span at rotor inlet section for different rotational speed, partial hub admission.

backside and consequently the cavity between the impeller and the stationary housing.

As reported by the authors in a previous work [14], there is a correlation between the nonuniformity index and the performance of the machine in different operating conditions. Higher alpha index values correspond to lower efficiency and vice versa when comparing partial shroud and partial hub admission conditions.

As shown in Figures 15(a)-15(b), index value in partial shroud case is always higher than partial hub: this leads to lower total-to-static efficiency only if the shroud limb is fed. This behaviour can be explained with the presence of a large

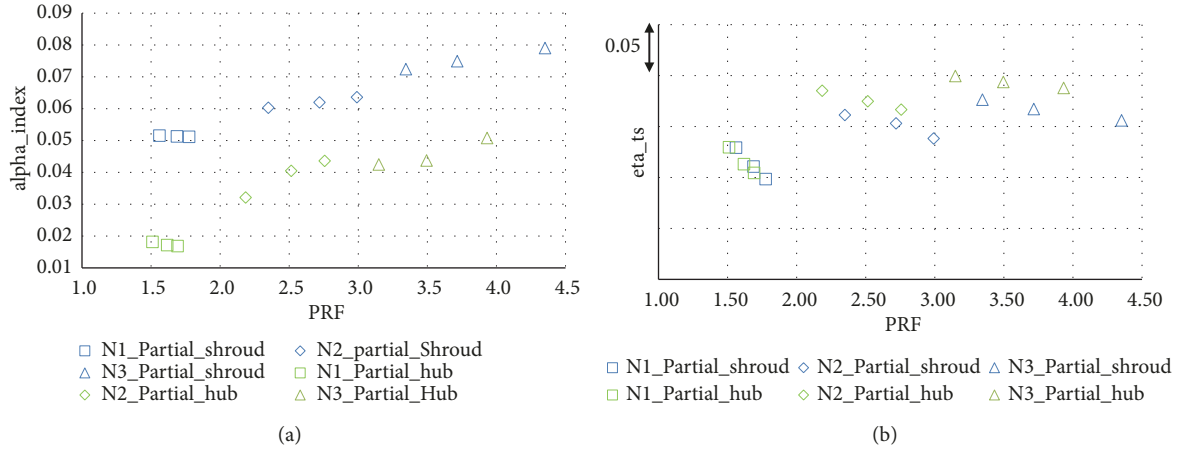


FIGURE 15: (a) Alpha index and (b) total-to-static efficiency vs PRF.

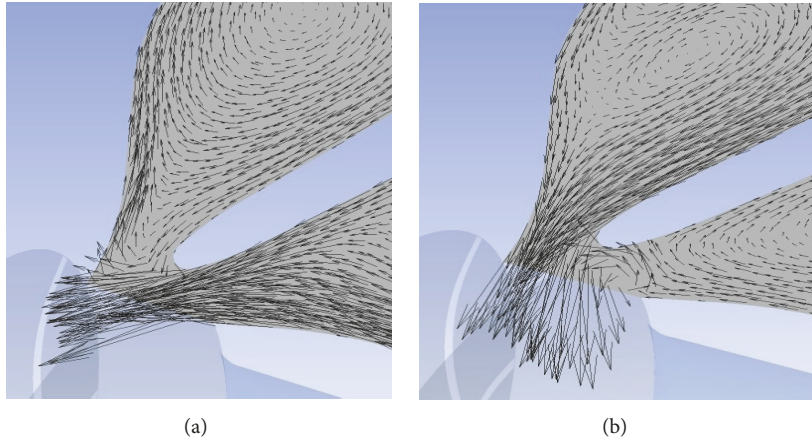


FIGURE 16: Velocity vectors at a volute cross section for (a) partial shroud and (b) partial hub admission.

recirculation zone in the not fed limb for partial shroud admission.

In Figures 16(a) and 16(b) velocity vectors on a volute cross section are compared for the two partial cases: recirculation appears in both situations; however this phenomenon is stronger when only the shroud branch is fed, leading to higher fluid-dynamic losses and performance worsening.

7. Backside Cavity Influence on Performance

7.1. Introduction. The rotor backside and its cavity have been introduced into the 3D CFD model in order to understand the effect of this detail on the turbine performance. The set of operating points (Table 4) have been simulated using the same numerical approach described before. The performance is tested by changing rotational speed and pressure ratio in three different admission conditions: full, partial shroud, and partial hub. As in the previous analysis total-to-static efficiency and MFP are considered for the comparison.

The presence of the cavity alters the flow structure at the rotor inlet so an additional performance index based on total pressure distributions has been introduced to correlate

the volute flow structure at the rotor inlet and the turbine performance.

7.2. Total Pressure Index. The total pressure distribution along the span (hub to shroud) at rotor inlet is considered. Since the total pressure is linked to the amount of energy obtainable from the stream tubes, a large spanwise variation of this quantity affects volute performance and rotor efficiency. As for the absolute flow angle α , the deviation with respect to mean value has been computed in the formulation of the total pressure index (see (9)).

$$\begin{aligned}
 P_{t \text{ index}} = & \left(\frac{1}{n.v. * \overline{p_t}} \right) * [|P_{t \ 5} - \overline{p_t}| + |P_{t \ 20} - \overline{p_t}| \\
 & + |P_{t \ 40} - \overline{p_t}| + |P_{t \ 60} - \overline{p_t}| + |P_{t \ 80} - \overline{p_t}| \\
 & + |P_{t \ 95} - \overline{p_t}|] \quad (9)
 \end{aligned}$$

$\overline{p_t}$ is the mean value along the span; $p_{t \ n}$ is the total pressure value at the corresponding n-th span percentage position. Unlike α_{index} local deviations from mean value are not weighted with span position, because backside cavity

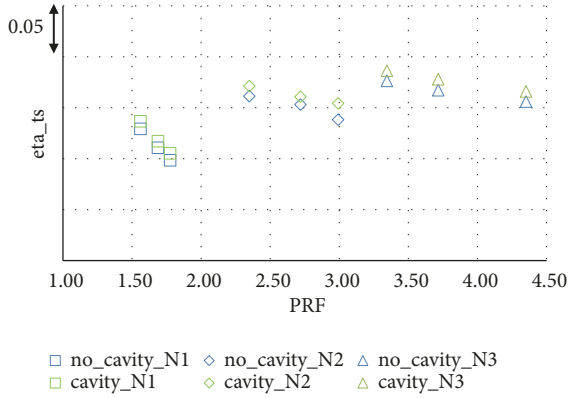


FIGURE 17: Total-to-static efficiency vs PRF comparison, partial shroud admission.

effects on flow field are concentrated on hub side and hence a formulation similar to (8) would have decreased total pressure nonuniformity influence in that specific zone. The definition of this new index did not replace α_{index} , which remains valid for volute performance evaluation but improves the description of flow nonuniformities at rotor inlet in case of backside cavity.

7.3. Comparison between Cases with or without Rotor Backside Cavity. The set of simulations (Table 4) has been repeated with rotor backside cavity included in the 3D model. Since pressure boundary conditions are kept the same, overall mass flow does not change significantly with respect to the cases simulated without cavity, even in partial admission conditions.

The performance parameter chosen to compare the cases with or without backside cavity is the total-to-static efficiency. The operating points in partial shroud admission are considered first.

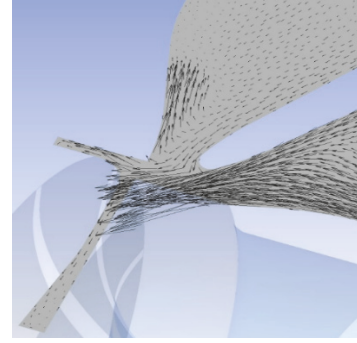
As reported in Figure 17, the presence of the backside cavity seems to have a positive influence on the turbine efficiency when only the shroud limb is fed: η_{ts} tends to be higher in case of turbine model with cavity. This behaviour is explained by the flow structure in the volute.

A volute cross section (with backside cavity) is shown in Figures 18(a)-18(b) with velocity vectors projected onto it.

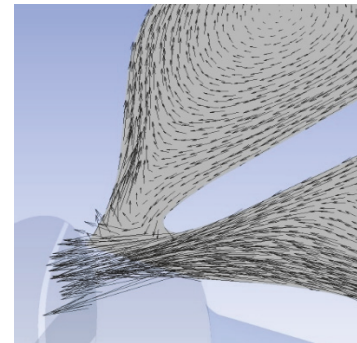
A qualitative assessment of the flow field leads to the conclusion that the cavity reduces the strong flow recirculation into the not fed limb typical of partial shroud admission.

Total pressure distribution from hub to shroud at rotor inlet section has been plotted for both cavity and no-cavity cases. Values are reported in nondimensional form (Figures 19(a)-19(b)) as a ratio between local and average spanwise value for all the rotational speeds considered. It can be noticed that when backside cavity is not included into the CFD model the total pressure values at the hub region (close to zero span) are generally lower than those registered with cavity; this difference is more evident at high rotational speeds.

In Figure 20 the total pressure index has been plotted against the PRF. It can be noticed that $p_{t\ index}$ trends correlate with the corresponding curves of total-to-static efficiency.

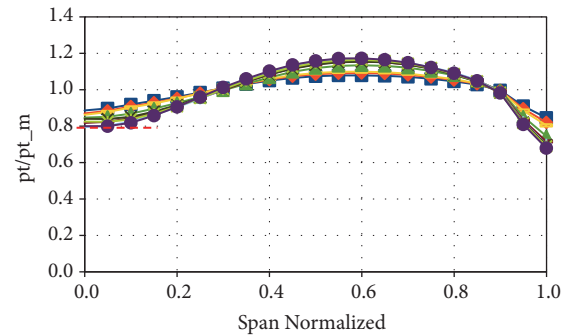


(a)

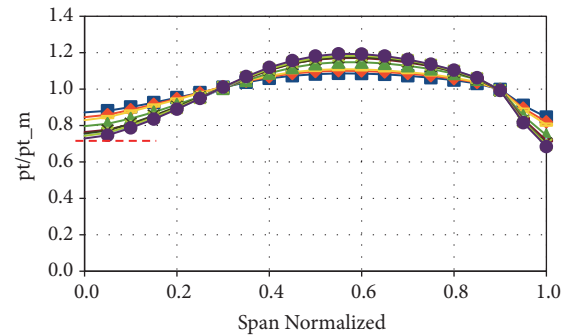


(b)

FIGURE 18: Velocity vectors in a volute cross section for partial shroud admission (a) with the backside cavity and (b) without it.



(a)



(b)

FIGURE 19: Total pressure ratio vs span, partial shroud admission, (a) with cavity and (b) without cavity.

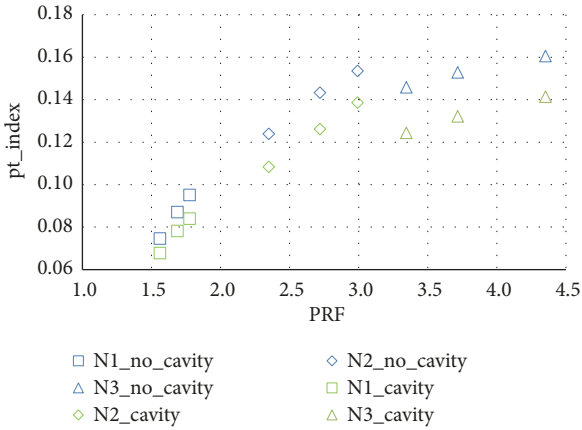


FIGURE 20: pt_index vs PRF comparison, partial shroud admission.

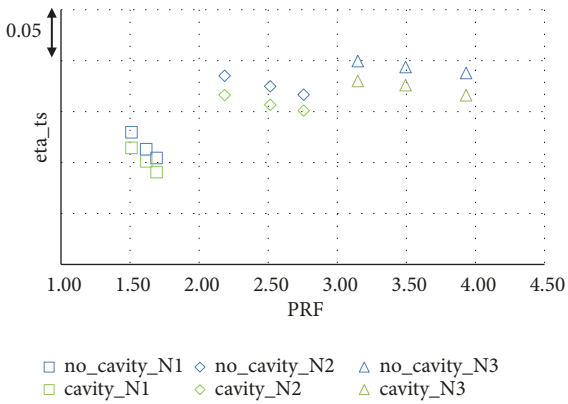


FIGURE 21: Total-to-static efficiency vs PRF comparison, partial hub admission.

Higher values of the index correspond to lower values of efficiency and vice versa (compare Figures 17–20).

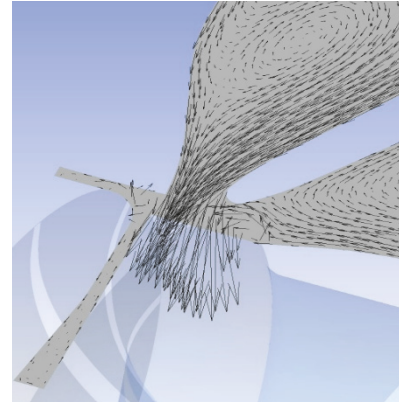
The set of operating conditions in partial hub admission are now discussed.

If only the hub limb is fed the influence of the backside cavity gives lower total-to-static efficiency values than without cavity, as displayed in Figure 21.

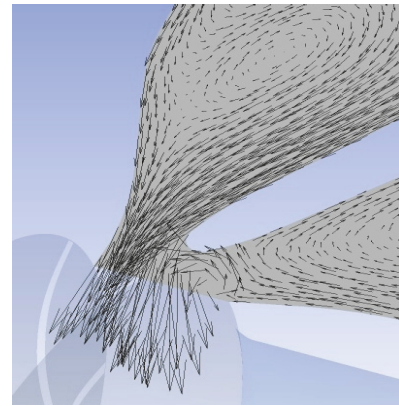
In these cases the presence of the cavity tends to slightly increase the flow recirculation into the not fed volute branch. In Figure 22 the projected velocity vectors on a volute cross section show the abovementioned effect (consider vector magnitude in the not powered limb, the shroud side).

The total pressure hub-to-shroud distributions are reported for all the rotational speeds in Figures 23(a)-23(b) with and without cavity, respectively. The local values of total pressure referred to the corresponding averaged spanwise value (p_{tm}) are shown. It can be noticed that, unlike in partial shroud conditions (Figure 21), the total pressure is higher in the hub zone without the cavity; more losses occur in the cavity case.

The total pressure index distributions are shown in Figure 24.

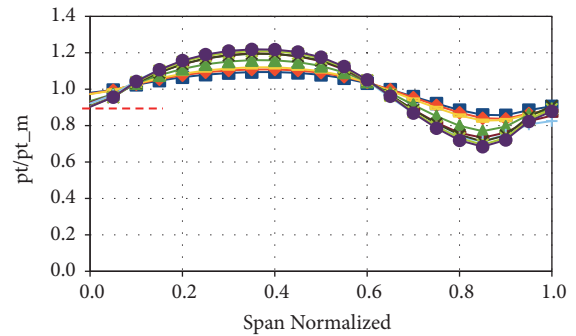


(a)

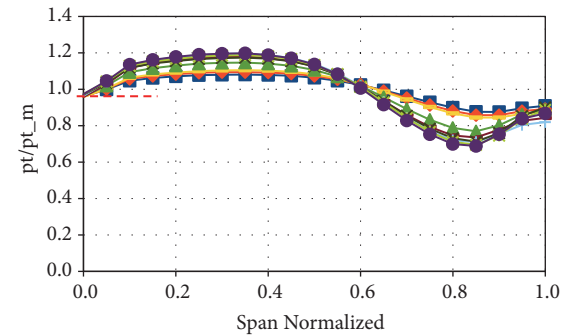


(b)

FIGURE 22: Velocity vectors in a volute cross section for partial hub admission (a) with backside cavity and (b) without it.



(a)



(b)

FIGURE 23: Total pressure ratio vs span, partial hub admission, (a) with cavity and (b) without cavity.

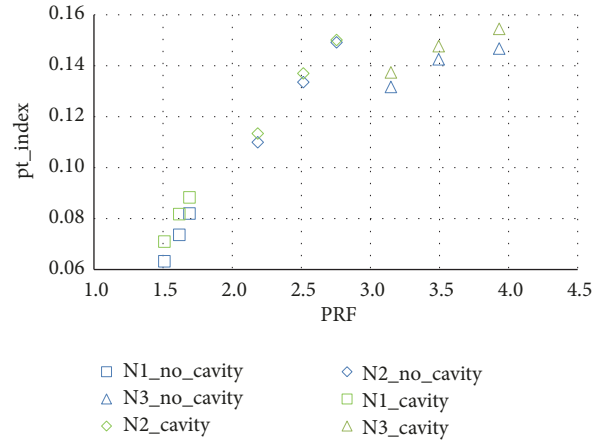


FIGURE 24: pt_{index} vs PRF, partial hub admission.

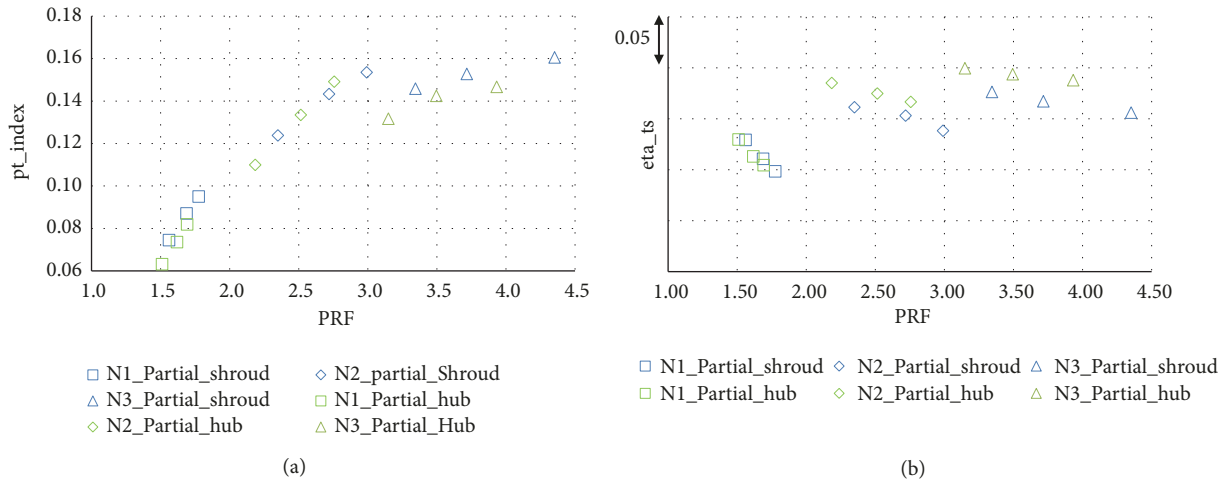


FIGURE 25: Performance comparison between partial shroud and partial hub without backside cavity: (a) total pressure index and (b) total-to-static efficiency vs PRF.

The good link between $P_t index$ and total-to-static efficiency values is confirmed. Higher values of the index (with cavity in this case) correlate to lower values of efficiency (compare Figures 23-24).

A comparison between turbine performance in partial ‘shroud’ and ‘hub’ admission has suggested the use of the total pressure index. The cases with or without the backside cavity are therefore considered separately.

In the following it can be noticed that the above index agrees with the efficiency trends (see Figures 25(a)-25(b)): partial shroud admission leads to worse performance than partial hub case.

The introduction of the cavity greatly affects turbine performance in partial admission, up to the point that efficiency trends are reversed (compare Figures 25(b)-26(b)): the radial turbine model with cavity has better performance in partial shroud admission rather than in partial hub.

The abovementioned trend is well correlated to the total pressure index variation.

8. Conclusions

In the present paper a CFD methodology for the performance analysis of a twin scroll radial turbine has been set up. Simulations were performed in both full and partial admission, considering three different rotational speeds and, for each of them, three different pressure ratios were tested. The simulated performance has then been compared to available experimental data in order to validate the model. It emerged that values of MFP from CFD are in good agreement with the reference experimental data and that the total-to-static isentropic efficiency calculated with the numerical model does not take into account the mechanical losses, leading to an overestimation of the experimental thermomechanical efficiency. The systematic application of the present can generate performance database useful for investigation on turbine performance or operating parameters [17].

The database from the CFD analysis has then been used to investigate the volute performance and to identify a parameter that could be employed for design purposes,

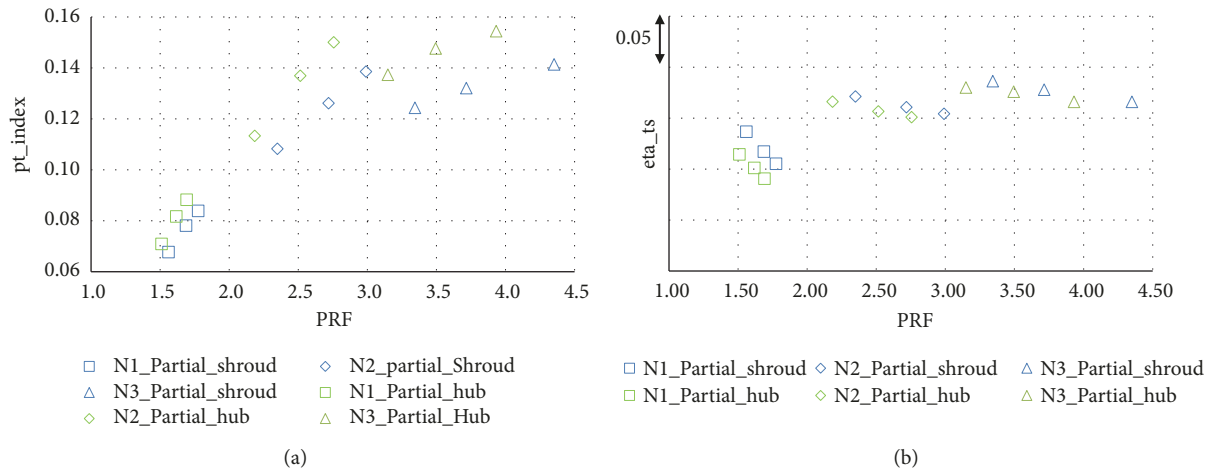


FIGURE 26: Performance comparison between partial shroud and partial hub with backside cavity: (a) total pressure index and (b) total-to-static efficiency.

especially for automatic design optimization. In order to increase the fidelity of the model, the rotor backside cavity has been included into the numerical model and the CFD database extended. The turbine performance at opposite partial admission conditions ('hub' or 'shroud') were compared with and without the backside cavity: different trends have been detected, highlighting the importance of the cavity in this specific volute configuration. The proposed performance index based on the total pressure spanwise distribution at the rotor inlet directly correlates to the total-to-static efficiency. The peculiar configuration studied, thanks to its strong geometrical asymmetry, has helped the detailed investigation of flow structures at partial admission and the introduction of flow distortion parameters that would be effective for the design optimization of volutes.

Nomenclature

A:	Area (m^2)
C_p :	Specific heat at constant pressure (J/kg K)
h:	Specific enthalpy (J/kg)
m:	Mass flow rate (kg/s)
N:	Turbine speed (rpm)
N_{red} :	Reduced turbine speed ($rpm/K^{0.5}$)
p:	Pressure (Pa)
p_{t_index} :	Total pressure index
r:	Radius (m)
Su:	Sutherland constant
T:	Temperature (K)
z_b :	Number of blades
α :	Flow angle in stationary frame (deg)
α_{index} :	Flow angle nonuniformity index
β :	Flow angle in relative frame (deg)
η :	Efficiency
μ :	Dynamic viscosity (kg/m s).

Subscripts

b:	Metal angle
ex:	Turbine exit

hub:	Hub volute inlet
is:	Isentropic
m:	Mean value
red:	Reduced
ref:	Reference values
sh:	Shroud volute inlet
t:	Total conditions
TM:	Thermomechanical
tot:	Overall
ts:	Total-to-static
1:	Turbine inlet
2:	Volute outlet/rotor inlet
3:	Rotor outlet.

Acronyms

MFP:	Mass flow parameter
MFR:	Mass flow ratio
PRF:	Pressure ratio flow
<i>n.v.</i> :	Number of span sampling points.

Data Availability

The data used to support the findings of this study have not been made available because of confidentiality issues. This is because the data are protected by industrial intellectual property and the research work has been possible only after an appropriate nondisclosure agreement.

Conflicts of Interest

The authors declare that they have no conflicts of interest.

References

- [1] C. Cravero, "A design methodology for radial turbomachinery: application to turbines and compressors," in *Proceedings of the ASME 2002 Joint U.S.-European Fluids Engineering Division Conference*, pp. 323–330, Montreal, Quebec, Canada, July 2002, paper FEDSM2002-31335.

- [2] C. Cravero, M. Marini, and A. Satta, "The design of a radial turbine for microgasturbine applications," in *Proceedings of the ASME/JSME 2003 4th Joint Fluids Summer Engineering Conference*, pp. 1323–1328, Honolulu, Hawaii, USA, July, 2003, FEDS2003-45417.
- [3] C. Cravero and M. Marini, "An integrated software procedure to support teaching of radial inflow turbine design," in *Proceedings of the ASME Turbo Expo 2007: Power for Land, Sea, and Air*, pp. 503–511, Montreal, Canada, May 2007, ASME Paper GT2007-27778.
- [4] M. S. Chiong, S. Rajoo, R. F. Martinez-Botas, and A. W. Costall, "Engine turbocharger performance prediction: one-dimensional modeling of a twin entry turbine," *Energy Conversion and Management*, vol. 57, pp. 68–78, 2012.
- [5] A. Romagnoli, C. D. Copeland, R. Martinez-Botas, M. Seiler, S. Rajoo, and A. Costall, "Comparison between the steady performance of double-entry and twin-entry turbocharger turbines," *Journal of Turbomachinery*, vol. 135, no. 1, 2013.
- [6] A. Dale and N. Watson, "Vaneless radial turbocharger turbine performance," *I Mech E Conference Publications (Institution of Mechanical Engineers)*, vol. C110/86, pp. 65–76, 1986.
- [7] V. De Bellis, S. Marelli, F. Bozza, and M. Capobianco, "1D simulation and experimental analysis of a turbocharger turbine for automotive engines under steady and unsteady flow conditions," *Energy Procedia*, vol. 45, pp. 909–918, 2014.
- [8] A. Romagnoli, R. F. Martinez-Botas, and S. Rajoo, "Steady state performance evaluation of variable geometry twin-entry turbine," *International Journal of Heat and Fluid Flow*, vol. 32, no. 2, pp. 477–489, 2011.
- [9] M. Cerdoun and A. Ghenaiet, "Characterization of a twin-entry radial turbine under pulsatile flow condition," *International Journal of Rotating Machinery*, vol. 2016, Article ID 4618298, 15 pages, 2016.
- [10] H. Raetz, J. Kammeyer, C. K. Natkaniec, and J. R. Seume, "Numerical investigation of aerodynamic radial and axial impeller forces in a turbocharger," in *Proceedings of the ASME 2011 Turbo Expo: Turbine Technical Conference and Exposition, GT2011-46360*, pp. 919–928, Canada, June 2011.
- [11] P. Newton, C. Copeland, R. Martinez-Botas, and M. Seiler, "An audit of aerodynamic loss in a double entry turbine under full and partial admission," *International Journal of Heat and Fluid Flow*, vol. 33, no. 1, pp. 70–80, 2012.
- [12] M. R. Shahhosseini, A. Hajilouy-Benisi, and M. Rajabian, "A numerical and experimental investigation of the effects of flow ratio on the flow and performance characteristics of a twin entry radial turbine," in *Proceedings of the ASME 2011 Turbo Expo: Turbine Technical Conference and Exposition, GT2011*, pp. 2139–2153, Canada, June 2011, ASME Paper GT2011-46308.
- [13] Y. Xue, M. Yang, R. F. Martinez-Botas, A. Romagnoli, and K. Deng, "Loss analysis of a mix-flow turbine with nozzled twin-entry volute at different admissions," *Energy*, vol. 166, pp. 775–788, 2019.
- [14] C. Cravero, M. La Rocca, and A. Ottonello, "Performance Characterization of a Twin Scroll Volute for Turbocharging Applications," in *Proceedings of the ASME Turbo Expo 2018: Turbomachinery Technical Conference and Exposition*, p. V02BT44A010, Oslo, Norway, ASME Paper GT2018-75522.
- [15] A. Ottonello, *CFD analysis of the performance of a twin entry radial turbine for turbocharging [Master, thesis]*, Mechanical Engineering, University of Genoa, 2017.
- [16] J. R. Serrano, P. Olmeda, A. Tiseira, L. M. García-Cuevas, and A. Lefebvre, "Theoretical and experimental study of mechanical losses in automotive turbochargers," *Energy*, vol. 55, pp. 888–898, 2013.
- [17] C. Cravero, D. De Domenico, and A. Ottonello, "Investigation on the degree of reaction in twin scroll radial turbines at different operating conditions for turbocharging applications," ASME Paper GT2019-90285, ASME Turbo Expo, Phoenix, Ariz, USA, 2019.



Hindawi

Submit your manuscripts at
www.hindawi.com

